JACS
JOURNAL OF THE AMERICAN CHEMICAL SOCIETY

pubs.acs.org/JACS

Communication

Counteranions in the Stimulation Solution Alter the Dynamics of Exocytosis Consistent with the Hofmeister Series

Xiulan He and Andrew G. Ewing*

Cite This: *J. Am. Chem. Soc.* 2020, 142, 12591−12595

Read Online

ACCESS | Metrics & More | Article Recommendations | Supporting Information

ABSTRACT: We show that the Hofmeister series of ions can be used to explain the cellular changes in exocytosis observed by single-cell amperometry for different counteranions. The formation, expansion, and closing of the membrane fusion pore during exocytosis was found to be strongly dependent on the counteranion species in solution. With stimulation of chaotropic anions (e.g., ClO_4^-), the expansion and closing time of the fusion pore are longer, suggesting chaotropes can extend the duration of exocytosis compared with kosmotropic anions (e.g., Cl^-). At a concentration of 30 mM, the two parameters (e.g., $t_{1/2}$ and t_{fall}) that define the duration of exocytosis vary with the Hofmeister series ($Cl^- < Br^- < NO_3^- \leq ClO_4^- < SCN^-$). More interestingly, fewer (e.g., N_{foot}/N_{events}) and smaller (e.g., I_{foot}) prespike events are observed when chaotropes are counterions in the stimulation solution, and the values can be sorted by the reverse Hofmeister series ($Cl^- \geq Br^- > NO_3^- > ClO_4^- > SCN^-$). Based on ion specificity, an adsorption-repulsion mechanism, we suggest that the exocytotic Hofmeister series effect originates from a looser swelling lipid bilayer structure due to the adsorption and electrostatic repulsion of chaotropes on the hydrophobic portion of the membrane. Our results provide a chemical link between the Hofmeister series and the cellular process of neurotransmitter release via exocytosis and provide a better physical framework to understand this important phenomenon.

Specific ion effects have attracted increasing scientific and technologic interests due to their broad applications in a wide range of fields such as biology,[1,2] colloids,[3] macromolecules,[4,5] nanomaterials,[6−9] two-phase interfaces,[10−12] ionic liquids,[13] and gels.[14] More interesting, there is a reoccurring trend of specific ion effects, the Hofmeister series, and it is also the earliest reported and the most studied.[15,16] Kosmotropic and chaotropic ion properties are observed in the species that span the Hofmeister series (e.g., $Cl^- < Br^- < NO_3^- < ClO_4^- < SCN^-$). These effects have been studied in biological systems (e.g., proteins,[17,18] lipids,[1,19] peptides,[20,21] biochannels,[22] enzymes[23,24]), physiochemical systems (e.g., colloids,[3] polymers[4,5]), and engineering systems (e.g., nanomaterials,[6−9] interfaces[10−12,25]). In addition to regulating the biological microenvironment (e.g., pH),[26,27] there is an ion-species-dependent effect of these anions on the activity of bioenzymes, which is expected to be used in the design of antiinfactives.[28−31] The permeability of inorganic anions, across the blood−brain barrier differs along the Hofmeister series.[32] Especially, Br^- has been used to treat epilepsy.[33,34] Moreover, the biological process of exocytosis has been studied to examine the effect of ions on release.[35−37] However, these studies were focused on bivalent cations (e.g., Ca^{2+}, Ba^{2+}, Sr^{2+}, Zn^{2+}) used to depolarize the membrane.[38−41] The influence of the Hofmeister anion series on exocytosis has not been investigated to date, although several papers have reported that these ions should strongly influence the structure or behavior of specific cellular components.[19−22]

In this paper, we studied the effects of the Hofmeister monovalent anion series on the exocytotic release of catecholamines from isolated adrenal chromaffin cells (see Supporting Information S1). For these studies, single-cell amperometry (SCA) was used to monitor exocytosis at the top of individual cells in culture. Exocytosis was triggered by stimulating the adrenal chromaffin cells with a 30 s 30 mM K^+ solution which included different counterions (i.e., Cl^-, Br^-, NO_3^-, ClO_4^-, or SCN^-), eventually leading to a train of peaks in the amperometric recording. Interestingly, it appears that K^+ stimulation with different counterions rapidly modulates the exocytosis process in a manner that is completely consistent with the Hofmeister series. Analysis of the exocytotic release peaks reveals that the counteranions in the stimulation solution regulate the fusion pore geometry, the duration of its opening, and closure.

Potassium stimulation of the cells with different counteranions appears to influence the exocytotic ability by chaotropic effects. Typical SCA amperometric traces obtained for exocytosis are shown in Figure 1 (left). Each trace represents a train of current transients following each stimulus, in which each current transient corresponds to a single vesicle release event. Several parameters that define the exocytosis process can be obtained from each individual exocytotic event (Figure S1), including I_{max}, the peak amplitude, $t_{1/2}$, the half peak width, t_{rise}, the 25−75% of rise time, t_{fall}, the 75−25% of fall time. The corresponding average peaks obtained from the typical traces for stimulation with 30 mM K^+ and Cl^-, Br^-

Received: May 14, 2020
Published: June 29, 2020

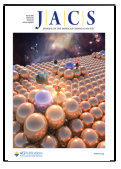

https://dx.doi.org/10.1021/jacs.0c05319
J. Am. Chem. Soc. 2020, 142, 12591−12595

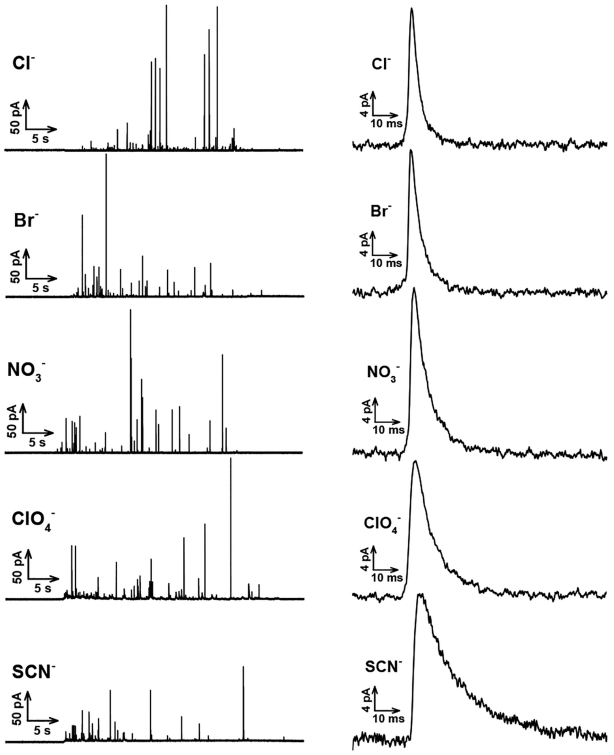

Figure 1. Left: Typical traces obtained from 30 mM K^+ stimulated chromaffin cells, including different counter-anions (e.g., Cl^-, Br^-, NO_3^-, ClO_4^-, SCN^-). Right: Average peaks obtained from the corresponding typical traces.

NO_3^-, ClO_4^-, and SCN^- as counterions are also shown in Figure 1 (right panels), showing that stimulus by kosmotropic counterions (e.g., Cl^-) leads to narrower exocytosis events, whereas stimulus by other chaotropic counterions (e.g., ClO_4^-) leads to broader or longer-lasting events.

To further study the effects of monovalent anionic counterions on exocytosis, the peak parameters obtained from the different counterions used during stimulation were analyzed. As previously reported,[42] the distribution of the exocytotic parameters is asymmetric and strongly deviates from Gaussian behavior, hence we chose the median for statistical analysis. The peak parameters for the main release events are summarized and analyzed in Figure 2 (p values are listed in Tables S1–S4). As shown in Figure 2A–C, a significant increase in the value of t_{rise}, $t_{1/2}$, and t_{fall} is observed after K^+ stimulation including chaotropic counterions (e.g., ClO_4^-), compared with the stimulation including kosmotropic counterions (e.g., Cl^-). This implies that the opening and closing of the fusion pore after stimulation in the presence of chaotropes (e.g., ClO_4^-) has been decelerated and the pore stays open for a longer time compared to kosmotropes (e.g., Cl^-) in the cell stimulation buffer.[43−45] Moreover, the event duration (i.e., $t_{1/2}$, t_{fall}) ranged over the entire Hofmeister series ($Cl^- < Br^- < NO_3^- \leq ClO_4^- < SCN^-$). As shown in Figure 2D, when cells are stimulated with high potassium and the counterion is moved from a kosmotrope (e.g., Cl^-) to a chaotrope (e.g., ClO_4^-), a significant increase in I_{max} for exocytosis is observed with the exception of SCN^-. Correspondingly, the number of molecules ($N_{molecules}$) is summarized in Figure S2A (p values are listed in Table S5). As the counteranions were changed only in the stimulation solution, we assume there is no effect

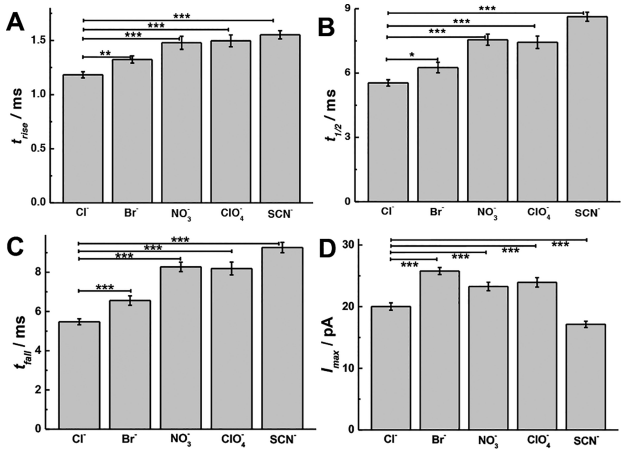

Figure 2. Scheme showing the peak analysis, comparisons of (A) t_{rise}, (B) $t_{1/2}$, (C) t_{fall}, and (D) I_{max} from SCA with chromaffin cells (n = 30) stimulated by 30 mM K^+ including different counteranions (e.g., Cl^-, Br^-, NO_3^-, ClO_4^-, and SCN^-). Pairs of data sets were compared with t test; ***, $p < 0.001$; **, $p < 0.01$; *, $p < 0.05$.

on the composition of vesicles and their content inside the cells during this acute application. We also studied the number of events and found there is little difference between counterions (Figure S2B, p values are listed in Table S6). Figure S2C,D is the log-normal frequency histograms of $N_{molecules}$ released per event, which provides a near-Gaussian distribution with similar standard deviation but different mean values for the distributions.

Exocytosis originates from the fusion of the cell and vesicle membranes.[35,46,47] Therefore, the structure and composition of both the cell and vesicle membranes (e.g., lipid bilayer, lipid rafts and biochannels) are closely related to the dynamic process of exocytosis.[46,47] To explain the exocytotic Hofmeister series data, we propose an adsorption−repulsion mechanism. The model in Figure 3A suggests a mechanism where the kosmotropes (e.g., Cl^-), which are believed to be

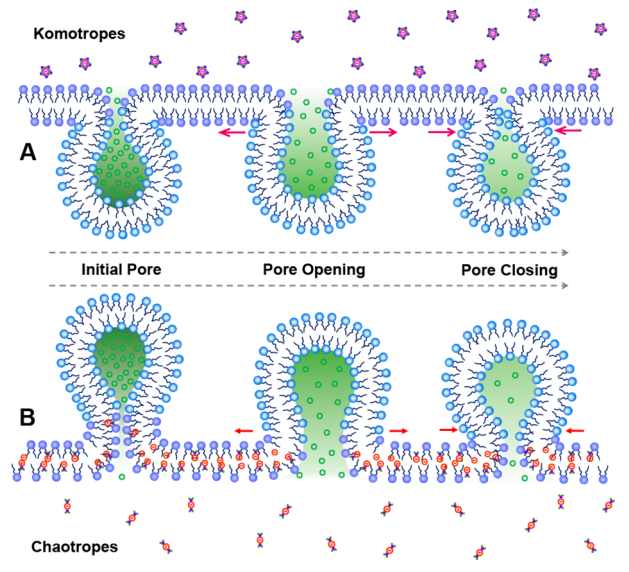

Figure 3. Illustration of a proposed adsorption-repulsion mechanism, showing chaotropic anions that adsorb on the hydrophobic part of the lipid layer by chaotropic effects leading to a swollen lipid bilayer and loosening of the structure of the lipid layer by electrostatic repulsion.

https://dx.doi.org/10.1021/jacs.0c05319
J. Am. Chem. Soc. 2020, 142, 12591−12595

"water structure makers", are strongly hydrated (i.e., $\Delta_{hyd}Cl^-$ = −419 kJ/mol, the hydration enthalpy of Cl^-) and have stabilizing and salting-out effects on proteins and macromolecules likely to be in the membrane.[2,8,48,49] Hence, the kosmotropes prefer to combine with H_2O rather than entering the lipid bilayer. On the other hand, chaotropes (Figure 3B) hold fewer H_2O molecules and have a less-structured hydration shell (e.g., ClO_4^-, $\Delta_{hyd}ClO_4^-$ = −263 kJ/mol) and are known to destabilize folded proteins via a salting-in behavior.[2,8,48,49] The chaotropes are then more hydrophobic and prefer the bilayer interior inducing lipid bilayer swelling, explained by chaotropic effects or hydrophobic interaction.[19,50−52] A "cone-shape" species results if we treat the single lipid molecule and the ions surrounded it as a whole, and when the cell membrane has more conical phospholipids, this slows exocytosis.[39] Then, electrostatic repulsion between the penetrating chaotropic anions and lipid headgroups leads to a change in the headgroup tilt and a looser lipid bilayer, which also slows down exocytosis.[53] Therefore, these two factors can both increase the duration of exocytosis leading to a range of event durations (i.e., $t_{1/2}$, t_{fall}) related to the Hofmeister series (Cl^- < Br^- < NO_3^- ≤ ClO_4^- < SCN^-). However, there are two opposing effects on I_{max} induced by "cone-shape" lipids (e.g., decreasing I_{max}) and looser lipid (e.g., increasing I_{max}), respectively.[39,53] Thus, we assume the magnitude of I_{max} is controlled by the difference in the two factors and does not in this case exactly follow the Hofmeister series. Although anionic effects could also alter the pore dynamics caused by SNARE proteins, we deliberately only introduce the different counteranions in the stimulation solution, so we assume there is only time for extracellular effect on the cell membrane. As the SNARE proteins are internal to the cell, we assume there is a minimal effect here.

To further confirm the rationale of the proposed adsorption−repulsion mechanism, the prespike feet (PSF), which are thought to be caused by the initial formation and stabilization of the membrane fusion pore, were examined. To prevent issues with poor signal-to-noise ratios, only peaks with a foot current (I_{foot}) larger than 2 pA were used for analysis. The relation between the PSF and the initial fusion pore has been established and widely applied.[54−56] The parameters for the PSF were analyzed according to the procedure presented in Figure S1. As shown in Figure 4 (p values are listed in Tables S7−S10), there is an inhibitory effect on the PSF when chaotropic counterions are present. There are fewer events with PSF (i.e., the probability of PSF, N_{foot}/N_{events}, Figure 4A), smaller feet (i.e., I_{foot}, Figure 4B; the number of molecules in foot, $N_{molecules}$ in foot, Figure 4C), and shorter events (i.e., t_{foot}, Figure 4D) for cells stimulated with chaotropic counterions (e.g., ClO_4^-) than for the kosmotropic counterions (e.g., Cl^-) in the stimulation buffer. The magnitude of these effects, in fact, follows the reverse Hofmeister series (Cl^- ≥ Br^- > NO_3^- > ClO_4^- > SCN^-). The smaller percentage of feet with chaotropic species might be affected by the signal cutoff for foot detection, but we also see significant difference even if we use no cutoff, where there is more background (Figure S3).

It has been demonstrated that I_{foot} is only related by the geometric parameters of the fusion pore (i.e., I_{foot} is proportional to R_{pore}^2/L_{pore}, where R_{pore} and L_{pore} are the radius and length of the initial pore) with an assumption that there is a constant catecholamine concentration in chromaffin cell vesicles.[57] This further suggests that chaotropic counterions influence the initial pore so that fewer molecules are released, and this could be via a smaller and longer pore. We hypothesize that cone-shape lipids in chaotrope-induced swelling of cell membranes favor stalk formation,[47] which decreases I_{foot} along the Hofmeister series. However, the stability of the pore (i.e., t_{foot}) is controlled by local molecular factors (e.g., SNARE proteins) and cell membrane physiochemical features (e.g., curvature).[58] Thus, we assume there are two adverse effects to make a small difference on t_{foot} between counteranions, in which outer "cone-shape" and looser bilayer increase t_{foot}, and inner "cone-shape" lipid decreases t_{foot}, respectively.[53,59]

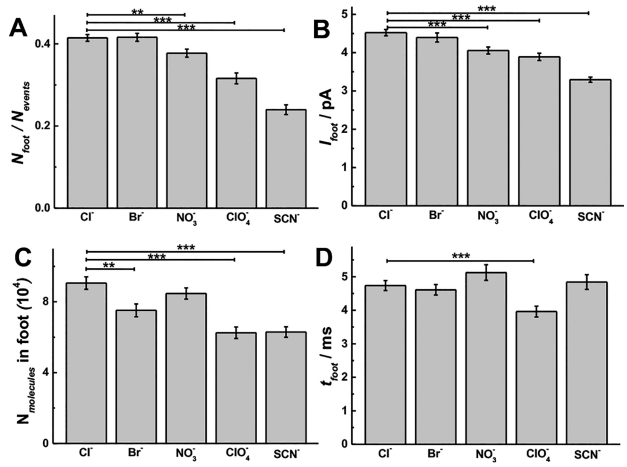

Figure 4. Foot parameters obtained from SCA with chromaffin cells (n = 30) stimulated by 30 mM K^+ solution including different counteranions (e.g., Cl^-, Br^-, NO_3^-, ClO_4^-, and SCN^-): (A) N_{foot}/N_{events}, (B) I_{foot} and (C) $N_{molecules}$ in foot, and (D) t_{foot}. Pairs of data sets were compared with t test; ***, p < 0.001; **, p < 0.01; *, p < 0.05.

We used adrenal chromaffin cells to study the effects of the monovalent anionic Hofmeister series on exocytotic release by SCA, showing a novel trend in exocytosis dynamics. The cellular response follows the Hofmeister series for the anionic counterions to potassium ion stimulation. The probability of PSF, the magnitude of I_{foot}, and the duration of exocytosis events depend on the counteranions according to their position in the Hofmeister series. Interestingly, the magnitude of dynamic exocytosis parameters (e.g., $t_{1/2}$, and t_{fall}) follows the Hofmeister series order (Cl^- < Br^- < NO_3^- ≤ ClO_4^- < SCN^-), but, in contrast, the probability of PSF and the magnitude of I_{foot} follow an anti-Hofmeister series order (Cl^- ≥ Br^- > NO_3^- > ClO_4^- > SCN^-). We propose a mechanism based on adsorption−repulsion, in which chaotropic anions enter the lipid bilayer and adsorb on the hydrophobic part via chaotropic effects, resulting in a loosening of the lipid structure from electrostatic repulsion. Our results provide a link between the Hofmeister series and the processes that regulate membrane structure and neurotransmitter release. We believe that our results are of importance for further progress in understanding the role of ion specificity, which manifests itself in many physicochemical and biological phenomena.

■ ASSOCIATED CONTENT

Supporting Information

The Supporting Information is available free of charge at https://pubs.acs.org/doi/10.1021/jacs.0c05319.

Experimental details, additional figures and tables (PDF)

https://dx.doi.org/10.1021/jacs.0c05319
J. Am. Chem. Soc. 2020, 142, 12591−12595

AUTHOR INFORMATION

Corresponding Author

Andrew G. Ewing − *Department of Chemistry and Molecular Biology, University of Gothenburg, 41296 Gothenburg, Sweden;* orcid.org/0000-0002-2084-0133; Email: andrew.ewing@chem.gu.se

Author

Xiulan He − *Department of Chemistry and Molecular Biology, University of Gothenburg, 41296 Gothenburg, Sweden*

Complete contact information is available at: https://pubs.acs.org/10.1021/jacs.0c05319

Notes

The authors declare no competing financial interest.

ACKNOWLEDGMENTS

We acknowledge support from the European Research Council (ERC Advanced Grant), the Knut and Alice Wallenberg Foundation in Sweden, the Swedish Research Council (VR), and the US National Institutes of Health (NIH). We would like to thank Dalsjöfors Kött AB, Sweden, and their employees for their kind help with providing the bovine adrenal glands.

REFERENCES

(1) Lo Nostro, P.; Ninham, B. W. Hofmeister Phenomena: An Update on Ion Specificity in Biology. *Chem. Rev.* **2012**, *112*, 2286−2322.

(2) Okur, H. I.; Hladílková, J.; Rembert, K. B.; Cho, Y.; Heyda, J.; Dzubiella, J.; Cremer, P. S.; Jungwirth, P. Beyond the Hofmeister Series: Ion-Specific Effects on Proteins and Their Biological Functions. *J. Phys. Chem. B* **2017**, *121*, 1997−2014.

(3) Kunz, W. Specific Ion Effects in Colloidal and Biological Systems. *Curr. Opin. Colloid Interface Sci.* **2010**, *15*, 34−39.

(4) Zhang, Y.; Cremer, P. S. Interactions between Macromolecules and Ions: the Hofmeister Series. *Curr. Opin. Chem. Biol.* **2006**, *10* (6), 658−663.

(5) Bruce, E. E.; Bui, P. T.; Rogers, B. A.; Cremer, P. S.; van der Vegt, N. F. A. Nonadditive Ion Effects Drive Both Collapse and Swelling of Thermoresponsive Polymers in Water. *J. Am. Chem. Soc.* **2019**, *141*, 6609−6616.

(6) Chilivery, R.; Begum, G.; Chaitanya, V.; Rana, R. K. Tunable Surface Wrinkling by a Bio-Inspired Polyamine Anion Coacervation Process that Mediates the Assembly of Polyoxometalate Nanoclusters. *Angew. Chem., Int. Ed.* **2020**, *59*, 8160−8165.

(7) Li, K.; Yang, J.; Gu, J. Salting-in Species Induced Self-Assembly of Stable MOFs. *Chem. Sci.* **2019**, *10*, 5743−5748.

(8) Assaf, K. I.; Nau, W. M. The Chaotropic Effect as an Assembly Motif in Chemistry. *Angew. Chem., Int. Ed.* **2018**, *57*, 13968−13981.

(9) Mittal, N.; Benselfelt, T.; Ansari, F.; Gordeyeva, K.; Roth, S. V.; Wågberg, L.; Söderberg, L. D. Ion-Specific Assembly of Strong, Tough, and Stiff Biofibers. *Angew. Chem., Int. Ed.* **2019**, *58*, 18562−18569.

(10) Luo, Z.-X.; Xing, Y.-Z.; Ling, Y.-C.; Kleinhammes, A.; Wu, Y. Electroneutrality Breakdown and Specific Ion Effects in Nano-confined Aqueous Electrolytes Observed by NMR. *Nat. Commun.* **2015**, *6*, 6358−6366.

(11) Jungwirth, P.; Tobias, D. J. Specific Ion Effects at the Air/Water Interface. *Chem. Rev.* **2006**, *106* (4), 1259−1281.

(12) Levin, Y.; dos Santos, A. P.; Diehl, A. Ions at the Air-Water Interface: An End to a Hundred-Year-Old Mystery? *Phys. Rev. Lett.* **2009**, *103*, 257802.

(13) Constantinescu, D.; Weingärtner, H.; Herrmann, C. Protein Denaturation by Ionic Liquids and the Hofmeister Series: A Case Study of Aqueous Solutions of Ribonuclease A. *Angew. Chem., Int. Ed.* **2007**, *46*, 8887−8889.

(14) Du, R.; Hu, Y.; Hübner, R.; Joswig, J. O.; Fan, X.; Schneider, K.; Eychmüller, A. Specific Ion Effects Directed Noble Metal Aerogels: Versatile Manipulation for Electrocatalysis and Beyond. *Sci. Adv.* **2019**, *5*, No. eaaw4590.

(15) Hofmeister, F. Zur Lehre von der Wirkung der Salze. *Naunyn-Schmiedeberg's Arch. Pharmacol.* **1888**, *24*, 247−260.

(16) Mazzini, V.; Craig, V. S. J. Specific-Ion Effects in Non-Aqueous Systems. *Curr. Opin. Colloid Interface Sci.* **2016**, *23*, 82−93.

(17) Salis, A.; Ninham, B. W. Models and Mechanisms of Hofmeister Effects in Electrolyte Solutions, and Colloid and Protein Systems Revisited. *Chem. Soc. Rev.* **2014**, *43*, 7358−7377.

(18) Rembert, K. B.; Paterová, J.; Heyda, J.; Hilty, C.; Jungwirth, P.; Cremer, P. S. Molecular Mechanisms of Ion-Specific Effects on Proteins. *J. Am. Chem. Soc.* **2012**, *134*, 10039−10046.

(19) Sachs, J. N.; Woolf, T. B. Understanding the Hofmeister Effect in Interactions between Chaotropic Anions and Lipid Bilayers: Molecular Dynamics Simulations. *J. Am. Chem. Soc.* **2003**, *125*, 8742−8743.

(20) Wei, F.; Li, H.; Ye, S. Specific Ion Interaction Dominates over Hydrophobic Matching Effects in Peptide-Lipid Bilayer Interactions: The Case of Short Peptide. *J. Phys. Chem. C* **2013**, *117*, 26190−26196.

(21) Balos, V.; Marekha, B.; Malm, C.; Wagner, M.; Nagata, Y.; Bonn, M.; Hunger, J. Specific Ion Effects on an Oligopeptide: Bidentate Binding Matters for the Guanidinium Cation. *Angew. Chem., Int. Ed.* **2019**, *58*, 332−337.

(22) Gurnev, P. A.; Roark, T. C.; Petrache, H. I.; Sodt, A. J.; Bezrukov, S. M. Cation-Selective Channel Regulated by Anions According to Their Hofmeister Ranking. *Angew. Chem., Int. Ed.* **2017**, *56*, 3506−3509.

(23) Zhang, Y.; Cremer, P. S. The Inverse and Direct Hofmeister Series for Lysozyme. *Proc. Natl. Acad. Sci. U. S. A.* **2009**, *106* (36), 15249−15253.

(24) Somasundar, A.; Ghosh, S.; Mohajerani, F.; Massenburg, L. N.; Yang, T.; Cremer, P. S.; Velegol, D.; Sen, A. Positive and Negative Chemotaxis of Enzyme-Coated Liposome Motors. *Nat. Nanotechnol.* **2019**, *14*, 1129−1134.

(25) He, Z.; Xie, W. J.; Liu, Z. Q.; Liu, G. M.; Wang, Z. W.; Gao, Y. Q.; Wang, J. J. Tuning Ice Nucleation with Counterions on Polyelectrolyte Brush Surfaces. *Sci. Adv.* **2016**, *2*, No. e1600345.

(26) Salis, A.; Monduzzi, M. Not only pH. Specific Buffer Effects in Biological Systems. *Curr. Opin. Colloid Interface Sci.* **2016**, *23*, 1−9.

(27) Hani, F. M.; Cole, A. E.; Altman, E. The Ability of Salts to Stabilize Proteins In Vivo or Intracellularly Correlates with the Hofmeister Series of Ions. *Int. J. Biochem. Mol. Biol.* **2009**, *10* (3), 23−31.

(28) Huang, L.; Xuan, W.; Sarna, T.; Hamblin, M. R. Comparsion of Thiocyanate and Selenocyanate for Potentiation of Antimicrobial Photodynamic Therapy. *J. Biophotonics* **2019**, *12*, No. e201800092.

(29) Conner, G. E.; Wijkstrom-Frei, C.; Randell, S. H.; Fernandez, V. E.; Salathe, M. The Lactoperoxidase System Links Anion Transport to Host Defense in Cystic Fibrosis. *FEBS Lett.* **2007**, *581*, 271−278.

(30) Maresca, A.; Vullo, D.; Scozzafava, A.; Supuran, C. T. Inhibition of the Alpha- and Beta-Carbonic Anhydrases from the Gastric Pathogen Helycobacter Pylori with Anions. *J. Enzyme Inhib. Med. Chem.* **2013**, *28* (2), 388−391.

(31) Burghout, P.; Vullo, D.; Scozzafava, A.; Hermans, P. W. M.; Supuran, C. T. Inhibition of the β-Carbonic Anhydrase from *Streptococcus Pneumonia* by Inorganic Anions and Small Molecules: Towards Innovative Drug Design of Antiinfectives? *Bioorg. Med. Chem.* **2011**, *19*, 243−248.

(32) Breschi, G. L.; Cametti, M.; Mastropietro, A.; Librizzi, L.; Baselli, G.; Resnati, G.; Metrangolo, P.; de Curtis, M. Different Permeability of Potassium Salts across the Blood-Brain Barrier Follows the Hofmeister Series. *PLoS One* **2013**, *8* (10), No. e78553.

(33) Kodama, K.; Omata, T.; Watanabe, Y.; Aoyama, H.; Tanabe, Y. Potassium Bromide in the Treatment of Pediatric Refractory Epilepsy. *J. Child Neurol.* **2019**, *34* (10), 582−585.

(34) Caraballo, R.; Pasteris, M. C.; Fortini, P. S.; Portuondo, E. Epilepsy of Infancy with Migrating Focal Seizures: Six Patients Treated with Bromide. *Seizure* **2014**, *23* (10), 899−902.
(35) Pang, Z. P.; Südhof, T. C. Cell Biology of Ca^{2+}-Triggered Exocytosis. *Curr. Opin. Cell Biol.* **2010**, *22* (4), 496−505.
(36) Denda, M.; Fuziwara, S.; Inoue, K. Influx of Calcium and Chloride Ions into Epidermal Keratinocytes Regulates Exocytosis of Epidermal Lamellar Bodies and Skin Permeability Barrier Homeostasis. *J. Invest. Dermatol.* **2003**, *121* (2), 362−367.
(37) Camacho, M.; Machado, J. D.; Montesinos, M. S.; Criado, M.; Borges, R. Intragranular pH Rapidly Modulates Exocytosis in Adrenal Chromaffin Cells. *J. Neurochem.* **2006**, *96*, 324−334.
(38) García, A. G.; García-De-Diego, A. M.; Gandía, L.; Borges, R.; García-Sancho, J. Calcium Signaling and Exocytosis in Adrenal Chromaffin Cells. *Physiol. Rev.* **2006**, *86*, 1093−1131.
(39) Amatore, C.; Arbault, S.; Bouret, Y.; Guille, M.; Lemaître, F.; Verchier, Y. Regulation of Exocytosis in Chromaffin Cells by Trans-Insertion of Lysophosphatidylcholine and Arachidonic Acid into the Outer Leaflet of the Cell Membrane. *ChemBioChem* **2006**, *7*, 1998−2003.
(40) Shin, O.-H.; Rhee, J.-S.; Tang, J.; Sugita, S.; Rosenmund, C.; Südhof, T. C. Sr^{2+} Binding to the Ca^{2+} Binding Site of the Synaptotagmin 1 C_2B Domain Triggers Fast Exocytosis without Stimulating SNARE Interactions. *Neuron* **2003**, *37*, 99−108.
(41) Ren, L.; Pour, M. D.; Majdi, S.; Li, X.; Malmberg, P.; Ewing, A. G. Zinc Regulates Chemical-Transmitter Storage in Nanometer Vesicles and Exocytosis Dynamics as Measured by Amperometry. *Angew. Chem., Int. Ed.* **2017**, *56*, 4970−4975.
(42) Li, X.; Dunevall, J.; Ewing, A. G. Using Single-Cell Amperometry To Reveal How Cisplatin Treatment Modulates the Release of Catecholamine Transmitters during Exocytosis. *Angew. Chem., Int. Ed.* **2016**, *55*, 9041−9044.
(43) Trouillon, R.; Ewing, A. G. Actin Controls the Vesicular Fraction of Dopamine Released During Extended Kiss and Run Exocytosis. *ACS Chem. Biol.* **2014**, *9*, 812−820.
(44) Trouillon, R.; Ewing, A. G. Amperometric Measurements at Cells Support a Role for Dynamin in the Dilation of the Fusion Pore during Exocytosis. *ChemPhysChem* **2013**, *14*, 2295−2301.
(45) Amatore, C.; Oleinick, A. I.; Svir, I. Reconstruction of Aperture Functions during Full Fusion in Vesicular Exocytosis of Neurotransmitters. *ChemPhysChem* **2010**, *11*, 159−174.
(46) Jahn, R.; Fasshauer, D. Molecular Machines Governing Exocytosis of Synaptic Vesicles. *Nature* **2012**, *490*, 201−207.
(47) Salaün, C.; James, D. J.; Chamberlain, L. H. Lipid Rafts and the Regulation of Exocytosis. *Traffic* **2004**, *5*, 255−264.
(48) He, X.; Zhang, K.; Liu, Y.; Wu, F.; Yu, P.; Mao, L. Chaotropic Monovalent Anion-Induced Rectification Inversion at Nanopipettes Modified by Polyimidazolium Brushes. *Angew. Chem., Int. Ed.* **2018**, *57*, 4590−4593.
(49) Mazzini, V.; Craig, V. S.J. Specific-Ion Effects in Non-Aqueous System. *Curr. Opin. Colloid Interface Sci.* **2016**, *23*, 82−93.
(50) Petrache, H. I.; Zemb, T.; Belloni, L.; Parsegian, V. A. Salt Screening and Specific Ion Adsorption Determine Neutral-Lipid Membrane Interactions. *Proc. Natl. Acad. Sci. U. S. A.* **2006**, *103* (21), 7982−7987.
(51) Aroti, A.; Leontidis, E.; Dubois, M.; Zemb, T. Effects of Monovalent Anions of the Hofmeister Series on DPPC Lipid Bilayers Part I: Swelling and In-Plane Equations of State. *Biophys. J.* **2007**, *93* (5), 1580−1590.
(52) Garcia-Celma, J. J.; Hatahet, L.; Kunz, W.; Fendler, K. Specific Anion and Cation Binding to Lipid Membranes Investigated on a Solid Supported Membrane. *Langmuir* **2007**, *23* (20), 10074−10080.
(53) Majdi, S.; Najafinobar, N.; Dunevall, J.; Lovric, J.; Ewing, A. G. DMSO Chemically Alters Cell Membranes to Slow Exocytosis and Increase the Fraction of Partial Transmitter Released. *ChemBioChem* **2017**, *18*, 1898−1902.
(54) Amatore, C.; Arbault, S.; Bonifas, I.; Guille, M.; Lemaître, F.; Verchier, Y. Relationship between Amperometric Pre-Spike Feet and Secretion Granule Composition in Chromaffin Cells: An Overview. *Biophys. Chem.* **2007**, *129*, 181−189.
(55) Han, X.; Wang, C.-T.; Bai, J.; Chapman, E. R.; Jackson, M. B. Transmembrane Segments of Syntaxin Line the Fusion Pore of Ca^{2+}-Triggered Exocytosis. *Science* **2004**, *304*, 289−292.
(56) Chow, R. H.; von Rüden, L.; Neher, E. Delay in Vesicle Fusion Revealed by Electrochemical Monitoring of Electrochemical Monitoring of Single Secretory Events in Adrenal Chromaffin Cells. *Nature* **1992**, *356*, 60−63.
(57) Mosharov, E. V.; Sulzer, D. Analysis of Exocytotic Events Recorded by Amperometry. *Nat. Methods* **2005**, *2* (9), 651−658.
(58) Amatore, C.; Arbault, S.; Bonifas, I.; Guille, M. Quantitative Investigations of Amperometric Spike Feet Suggest Different Controlling Factors of the Fusion Pore in Exocytosis at Chromaffin Cells. *Biophys. Chem.* **2009**, *143*, 124−131.
(59) Zhang, Z.; Jackson, M. B. Membrane Bending Energy and Fusion Pore Kinetics in Ca^{2+}-Triggered Exocytosis. *Biophys. J.* **2010**, *98* (11), 2524−2534.

https://dx.doi.org/10.1021/jacs.0c05319
J. Am. Chem. Soc. 2020, 142, 12591−12595